Soft and hard diffraction at LHC

S.M. Troshin, N.E. Tyurin

Institute for High Energy Physics
Protvino, Moscow Region, 142280 Russia

Abstract

Interest and problems in the studies of diffraction at LHC are highlighted. Predictions for the global characteristics of proton-proton interactions at the LHC energy are given. Potential for the discovery of the antishadow scattering mode and its physical implications for soft and hard diffractive processes are discussed.

Introduction

During recent years CERN, DESY and FNAL have been producing interesting results on diffractive production in hadron and deep-inelastic processes [1]. Discovery of hard diffraction at CERN S$\bar{p}p$S [2] and diffractive events in the deep-inelastic scattering at HERA [3, 4] were among the most surprising results obtained recently. Significant fraction of high-t events among the diffractive events in deep-inelastic scattering and in hadron-hadron interactions were also observed at HERA [5] and Tevatron [6] respectively. These experimental findings have renewed interest in the experimental and theoretical studies of the diffractive production processes.

The understanding of the diffractive interactions plays fundamental role in the studies of a high-energy limit of the modern strong interaction theory — QCD. This field is most interesting one since there are no firmly established computational methods within QCD. However, the progress in understanding of high–energy basic features and the underlying dynamics of diffraction mechanism can be traced in recent theoretical papers (cf. review [7]).

There is no doubt that soft and hard diffractive processes should be measured at the LHC. The most global characteristic of a hadronic process is the total cross–section, and the most important problem here is the nature of the total–cross section rising energy dependence. There are various approaches which provide total cross-section increasing with energy, but the underlying microscopic mechanism leading to this increase remains obscure.

Besides elastic scattering (total and elastic cross-sections), it is important to measure the inelastic diffractive final states, jet production, hadron transverse momentum distribution, strange and charmed particle productions. The single diffraction dissociation is a most simple inelastic diffractive process, and studies of soft and hard final states in this process could become the next obvious step after elastic measurements. Such experiments could become crucial for understanding of the microscopic nature of driving mechanism called Pomeron, its possible parton structure, high-energy limit of strong interactions and approaching the asymptotia.

1 Where will asymptotics be seen?

The answer for the above question is still model-dependent, and no universal criterion exists. There are model parameterizations for the total cross-sections which use $\ln^2 s$ dependence for $\sigma_{tot}(s)$. This implies the saturation of the Froissart–Martin bound, and what is unnatural, presence of the asymptotical contributions already at the very moderate energies. On the other hand, the power-like parameterizations of $\sigma_{tot}(s)$ neglect the Froissart–Martin bound considering it as a matter of the very distant asymptopia.

It seems that both approaches are limited, and this reflects to some extent that the available energy range for the analysis of the experimental data is very limited too. For example, it is not clear whether the power–like energy dependence would obey unitarity bounds for the partial–wave amplitudes at the LHC energies.

Unitarity is an important principle and the unitarization procedure of some input power-like "amplitude" leads to the complicated energy dependence of $\sigma_{tot}(s)$ which can be approximated by the different functional forms depending on the particular energy range under consideration. These forms providing a good description of the experimental data in the limited energy range can have nothing to do with the true asymptotic dependence $\ln^2 s$. Definitely, unitarization will lead to this $\ln^2 s$ dependence, but only at $s \to \infty$.

Unitarity of the scattering matrix $SS^+ = 1$ implies the existence at high energies $s > s_0$ of the new scattering mode – antishadow one. This has been described in some detail (cf. [9] and references therein), and the most important feature of this mode is the self-damping of the contribution from the inelastic channels. We argue here that the antishadow scattering mode could be definitely revealed at the LHC energy and provide numerical estimations based on the U-matrix unitarization method [10].

2 Antishadow scattering at LHC

In the impact parameter representation the unitarity relation written for the elastic scattering amplitude $f(s,b)$ at high energies has the form

$$Imf(s,b) = |f(s,b)|^2 + \eta(s,b) \tag{1}$$

where the inelastic overlap function $\eta(s,b)$ is the sum of all inelastic channel contributions. It can be expressed as the sum of n–particle production cross–sections at a given impact parameter

$$\eta(s,b) = \sum_n \sigma_n(s,b). \tag{2}$$

The impact parameter b has a simple geometrical meaning as the distance in the transverse plane between the centers of the two colliding hadrons. Unitarity equation has two solutions for the case of pure imaginary amplitude:

$$f(s,b) = \frac{i}{2}[1 \pm \sqrt{1-4\eta(s,b)}]. \tag{3}$$

Eikonal unitarization

$$f(s,b) = \frac{e^{2i\delta(s,b)}-1}{2i} \tag{4}$$

with pure imaginary eikonal ($\delta = i\Omega/2$) corresponds to the choice of the particular solution of the unitarity equation with the minus sign.

In the U–matrix approach the form of the elastic scattering amplitude in the impact parameter representation is the following:

$$f(s,b) = \frac{U(s,b)}{1-iU(s,b)}. \tag{5}$$

$U(s,b)$ is the generalized reaction matrix, which is considered as an input dynamical quantity similar to eikonal function.

Inelastic overlap function is connected with $U(s,b)$ by the relation

$$\eta(s,b) = \frac{ImU(s,b)}{|1-iU(s,b)|^2}. \tag{6}$$

Construction of particular models in the framework of the U–matrix approach proceeds the common steps, i.e. the basic dynamics as well as the notions on hadron structure being used to obtain a particular form for the U–matrix. However, the two unitarization schemes (U–matrix and eikonal) lead to different predictions for the inelastic cross–sections and for the ratio of elastic to total cross-section. This ratio in the U–matrix unitarization scheme reaches its possible maximal value at $s \to \infty$, i.e. growth of the elastic cross–section is to be steeper than the growth of the inelastic cross–section beyond some threshold energy

$$\sigma_{el}(s) \sim \sigma_{tot}(s) \sim \ln^2 s, \quad \sigma_{inel}(s) \sim \ln s, \tag{7}$$

which reflects the fact that the bound for the partial–wave amplitude in the U–matrix approach (unitarity limit) is $|f| \leq 1$, while the bound for the case of imaginary eikonal is (black disk limit) is $|f| \leq 1/2$. When the amplitude exceeds the black disk limit (in central collisions at high energies), then the scattering at such impact parameters turns out to be of an antishadow nature. In this antishadow scattering mode the elastic amplitude increases with decrease of the inelastic channels contribution.

It is worth noting that the shadow scattering mode is considered usually as the only possible one. But two solutions of the unitarity equation have equal validity, and the antishadow scattering mode should not be excluded.

Appearance of the antishadow scattering mode is completely consistent with the basic idea that the particle production is the driving force for elastic scattering. Indeed, the imaginary part of the generalized reaction matrix is the sum of inelastic channel contributions:

$$ImU(s,b) = \sum_n \bar{U}_n(s,b), \tag{8}$$

where n runs over all inelastic states and

$$\bar{U}_n(s,b) = \int d\Gamma_n |U_n(s,b,\{\xi_n\}|^2 \tag{9}$$

where $d\Gamma_n$ is the n–particle element of the phase space volume. The functions $U_n(s,b,\{\xi_n\})$ are determined by the dynamics of $2 \to n$ processes. Thus, the quantity $ImU(s,b)$ itself is a shadow of the inelastic processes. However, unitarity leads to self–damping of the inelastic channels [11] and increase of the function $ImU(s,b)$ results in decrease of the inelastic overlap function $\eta(s,b)$ when $ImU(s,b)$ exceeds unity.

Let us consider the transition to the antishadow scattering mode [12]. With conventional parameterizations of the U–matrix, the inelastic overlap function increases with energies at modest values of s. It reaches its maximum value $\eta(s,b=0) = 1/4$ at some energy $s = s_0$ and beyond this energy the antishadow scattering mode appears at small values of b. The region of energies and impact parameters corresponding to the antishadow scattering mode is determined by the conditions $Imf(s,b) > 1/2$ and $\eta(s,b) < 1/4$. The quantitative analysis of the experimental data [13] gives the threshold value of energy: $\sqrt{s_0} \simeq 2$ TeV. This value is confirmed by the recent model considerations [14].

Thus, the function $\eta(s,b)$ becomes peripheral when energy is increasing. At such energies the inelastic overlap function reaches its maximum value at $b = R(s)$, where $R(s)$ is the interaction radius. So, beyond the transition threshold, there are two regions in impact parameter space: the central region of antishadow scattering at $b < R(s)$ and the peripheral region of shadow scattering at $b > R(s)$. The impact parameter dependence of the amplitude $f(s,b)$ and inelastic channel contribution $\eta(s,b)$ at $s > s_0$ are represented in Fig. 1.

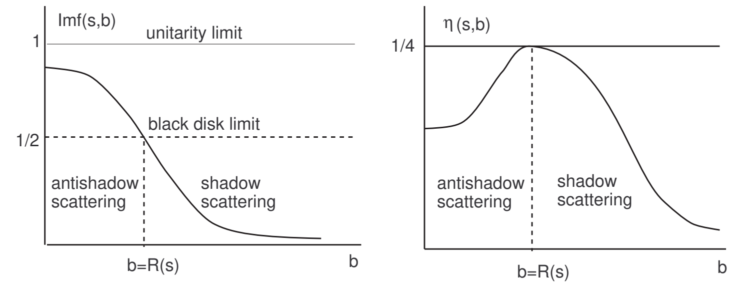

Figure 1: Shadow and antishadow scattering regions

The region of LHC energies is the one where antishadow scattering mode is to be presented. It will be demonstrated in the next section that this mode can be revealed directly measuring $\sigma_{el}(s)$ and $\sigma_{tot}(s)$, and not only through the analysis in impact parameter representation.

3 Transition to asymptotics

To get the numerical estimates, we shall use the following ansatz for the generalized reaction matrix

$$U(s,b) = ig\left[1+\alpha\frac{\sqrt{s}}{m_Q}\right]^N \exp(-Mb/\xi) \equiv ig(s)\exp(-Mb/\xi), \tag{10}$$

where $M = \sum_{q=1}^{N} m_Q$. Here m_Q is the mass of constituent quark, which is taken to be $0.35\ GeV$, N is the total number of valence quarks in the colliding hadrons, i.e. $N = 6$ for pp–scattering. The values for the other parameters were obtained in [13] and are the following: $g = 0.24$, $\xi = 2.5$, $\alpha = 0.56 \cdot 10^{-4}$. With these values of parameters, the model provides satisfactory description of the available experimental data for the forward elastic pp-scattering. To obtain the above explicit form for the function $U(s,b)$ we used chiral quark model for U–matrix [15] where $U(s,b)$ is chosen as a product of the averaged quark amplitudes

$$U(s,b) = \prod_{Q=1}^{N} \langle f_Q(s,b)\rangle \tag{11}$$

in accordance with the assumed quasi-independence of valence quark scattering. The b–dependence of the function $\langle f_Q\rangle$ related to the quark formfactor $F_Q(q)$ has a simple form $\langle f_Q\rangle \propto \exp(-m_Q b/\xi)$.

For the LHC energy $\sqrt{s} = 14\ TeV$ we have

$$\sigma_{tot} \simeq 230 \text{ mb} \tag{12}$$

and

$$\sigma_{el}/\sigma_{tot} \simeq 0.67. \tag{13}$$

Thus, the antishadow scattering mode could be discovered at LHC by measuring σ_{el}/σ_{tot} ratio which is greater than the black disc value 1/2.

However, the LHC energy is not in the asymptotic region yet; the total, elastic and inelastic cross-sections behave like

$$\sigma_{tot,el} \propto \ln^2\left[g\left(1+\alpha\frac{\sqrt{s}}{m_Q}\right)^N\right], \tag{14}$$

$$\sigma_{inel} \propto \ln\left[g\left(1+\alpha\frac{\sqrt{s}}{m_Q}\right)^N\right]. \tag{15}$$

Asymptotic behavior

$$\sigma_{tot,el} \propto \ln^2 s, \quad \sigma_{inel} \propto \ln s \tag{16}$$

is expected at $\sqrt{s} > 100\ TeV$.

Another predictions of the chiral quark model is decreasing energy dependence of the the cross-section of the inelastic diffraction at $s > s_0$. Decrease of diffractive production cross–section at high energies ($s > s_0$) is due to the fact that $\eta(s,b)$ becomes peripheral at $s > s_0$ and the whole picture corresponds to the antishadow scattering at $b < R(s)$ and to the shadow scattering at $b > R(s)$ where $R(s)$ is the interaction radius:

$$\frac{d\sigma_{diff}}{dM^2} \simeq \frac{8\pi g^* \xi^2}{M^2}\eta(s,0). \tag{17}$$

The parameter $g^* < 1$ is the probability of the excitation of a constituent quark during interaction. Diffractive production cross–section has the familiar $1/M^2$ dependence which is related in this model to the geometrical size of excited constituent quark.

At LHC energy $\sqrt{s} = 14\ GeV$, single diffractive inelastic cross-sections are limited by the value $\sigma_{diff}(s) \le 2.4$ mb.

The above predicted values for the global characteristics of pp – interactions at LHC differ from the most predictions of the other models. First of all, the total cross–section is predicted to be twice as big as the common predictions in the range 95-120 mb [16], and it even overshoots the existing cosmic ray data. However, extracting proton–proton cross sections from cosmic ray experiments is model dependent and far from straightforward (see, e.g. [17] and references therein). These experiments measure the attenuation lengths of showers initiated by the cosmic particles in the atmosphere and are sensitive to the model-dependent parameter called inelasticity. So the disagreement of a particular model with the cosmic ray measurements means that the data should be recalculated in the framework of this model, and in addition assumptions on the energy dependence of inelasticity should be involved also.

4 Angular structure of diffraction dissociation at LHC

Similarity between elastic and inelastic diffraction in the t-channel approach suggests that the latter one would have similar to behavior of the differential cross-section of elastic scattering. However, it cannot be taken for granted and e.g. transverse momentum distribution of diffractive events in the deep-inelastic scattering at HERA shows a power-like behavior without apparent dips [18]. Similar behavior was observed also in the hadronic diffraction dissociation process at CERN [2], where also no dip and bump structure was observed. Angular dependence of diffraction dissociation together with the measurements of the differential cross–section in elastic scattering would allow to determine the geometrical properties of elastic and inelastic diffraction, their similar and distinctive features and origin.

In the U-matrix approach the impact parameter amplitude of diffraction dissociation $F_{diff}(s,b,M)$ can be written in the pure imaginary case as a square root of the cross-section, i.e.

$$F_{diff}(s,b,M) = \sqrt{U_{diff}(s,b,M)}/[1+U(s,b)] \tag{18}$$

and the amplitude $F_{diff}(s,t,M)$ is

$$F_{diff}(s,t,M) = \frac{is}{\pi^2}\int_0^\infty bdbJ_0(b\sqrt{-t})\sqrt{U_{diff}(s,b,M)}/[1+U(s,b)]. \tag{19}$$

The corresponding amplitude $F_{diff}(s,t,M)$ can be calculated analytically. To do so, we continue the amplitudes $F_{diff}(s,\beta,M)$, $\beta=b^2$, to the complex β–plane and then $F_{diff}(s,t,M)$ can be represented as the sum of the pole contribution and the contribution of the cut [19]:

$$F_{diff}(s,t,M) = F_{diff,p}(s,t,M) + F_{diff,c}(s,t,M) \tag{20}$$

For elastic scattering amplitude $F(s,t)$ the pole and cut contributions are decoupled dynamically when $g(s)\to\infty$ at $s\to\infty$. Contribution of the poles determines the elastic amplitude in the region $|t|/s\ll 1$ $(t\neq 0)$. The amplitude in this region can be represented in a form of series over the parameter $\tau(\sqrt{-t})$:

$$F(s,t) = s\sum_{k=1}^{\infty}\tau^k(\sqrt{-t})\varphi_k[R(s),\sqrt{-t}], \tag{21}$$

where $\varphi_k[R(s),\sqrt{-t}]$ are the oscillating functions of the variable $\sqrt{-t}$. The parameter τ decreases exponentially with $\sqrt{-t}$:

$$\tau(\sqrt{-t}) = \exp(-\frac{2\pi\xi}{\tilde{M}}\sqrt{-t}).$$

This series reproduces diffraction peak and familiar dip-bump structure of the differential cross-section in elastic scattering. In the region of moderate t it is sufficient to take into account few or even one of the terms of series Eq. (21). The differential cross-section in this region has familiar Orear behavior.

The situation is different in the case of diffraction production. Instead of dynamical separation of the pole and cut contribution discussed above, we have a suppression of the pole contribution at high energies, since at fixed t

$$F_{diff,p} = O(s[g(s)]^{-\frac{M}{2\tilde{M}}}\ln^{1/2}g(s)),\quad F_{diff,c} = O(s[g(s)]^{-\frac{1}{2}}). \tag{22}$$

Therefore, at all t values we will have

$$F_{diff}(s,t,M)\simeq F_{diff,c}(s,t,M), \tag{23}$$

where

$$F_{diff,c}(s,t,M) \simeq ig^* g^{-1/2}(s)(1-\frac{t}{\bar{M}^2})^{-3/2}, \tag{24}$$

where $\bar{M} = (M - \tilde{M} - 1)/2\xi$. This means that the differential cross-section of the diffraction production will have smooth dependence on t with no apparent dips and bumps

$$\frac{d\sigma_{diff}}{dtdM^2} \propto (1-\frac{t}{\bar{M}^2})^{-3}. \tag{25}$$

It is interesting to note that at large values of $M \gg \tilde{M}$ the normalized differential cross-section $\frac{1}{\sigma_0}\frac{d\sigma}{dtdM^2}$ (σ_0 is the value of cross-section at $t=0$) will exhibit scaling behavior

$$\frac{1}{\sigma_0}\frac{d\sigma}{dtdM^2} = f(-t/M^2), \tag{26}$$

and explicit form of the function $f(-t/M^2)$ is the following

$$f(-t/M^2) = (1-4\xi^2 t/M^2)^{-3}. \tag{27}$$

This dependence is depicted on Fig. 2.

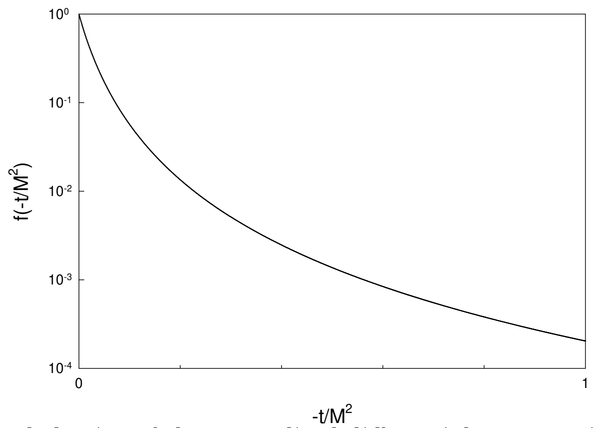

Figure 2: Scaling behavior of the normalized differential cross-section $\frac{1}{\sigma_0}\frac{d\sigma}{dtdM^2}$.

The above scaling was obtained in the model approach, however it might have a more general meaning.

The angular structure of diffraction dissociation processes given by Eq. (25) takes place at high energies, where $g(s) > 1$, while at moderate and low energies, where $g(s) \leq 1$, both contributions from poles and cut are significant. In this region

$$F_{diff}(s,t,M^2) = s\sum_{k=1}^{\infty} \tau^k(\sqrt{-t})\varphi_{diff,k}[R(s),\sqrt{-t},M^2], \tag{28}$$

where the parameter $\tau(\sqrt{-t})$ is the same as in the elastic case. Thus, at low energies the situation is similar to the elastic scattering, i.e. diffraction cone and possible dip-bump structure should be present in the region of small values of t, and behavior of the differential cross-section will be rather complicated and incorporates diffraction cone, Orear type and power-like dependencies.

However, at high energies a simple power-like dependence on t Eq. (25) is predicted. It was shown that the normalized differential cross-section has a scaling form and only depends on the ratio $-t/M^2$ at large values of M^2.

In fact, our comparative analysis of the poles and cut contributions has very little dependence on the form of a model of the U–matrix. This is why it has a more general meaning.

At the LHC energy the diffractive events with the masses as large as 3 TeV could be studied. It would be interesting to check this prediction at the LHC, where the scaling and simple power-like behavior of diffraction dissociation differential cross-section should be observed. Observation of such behavior would confirm the diffraction mechanism based on excitation of the complex hadronlike object - constituent quark. This mechanism can in principle explain angular structure of diffraction in the deep-inelastic scattering at HERA, where smooth angular dependence on the thrust transverse momentum was observed [18]. If it is the case, then diffraction in DIS at lower energies should manifest typical soft diffractive behavior with exponential peak at small t as it does in hadronic reactions. It would be interesting to check this at lower energies as well.

5 Discussions and conclusion

The main point of this note is to stress that the antishadow scattering mode at the LHC can be unambiguously detected measuring elastic to total cross section ratio, which is predicted to be greater than the black disc limit 1/2. The considered model predicts also the total cross section values significantly higher than those the conventional parameterizations provide. This feature of the total cross sections in this approach is in interrelation with the power law behavior of the differential cross sections of large angle scattering.

Thus, the studies of soft interactions at the LHC energies can lead to discoveries of fundamental importance. The genesis of hadron scattering with rising energy can be described as transition from the grey to black disc and eventually to black ring with the antishadow scattering mode in the center. It is worth noting that the appearance of the antishadow scattering mode at the LHC energy implies a somewhat unusual scattering picture. At high energies, the proton should be represented as a very loosely bounded composite system, and it appears that this system has a high probability to reinstate itself only in the central collisions, where all of its parts participate in the coherent interactions. Therefore the central collisions are responsible for elastic processes, while the peripheral ones, where only few parts of weekly bounded protons are involved, result in the production of the secondary particles. This leads to the peripheral impact parameter profile of the inelastic overlap function.

There could be envisaged various experimental configurations at the LHC; e.g. soft diffraction goes well to the interest of the TOTEM experiment, while hard diffractive final states can be measured by CMS detector and possible correlations between the features of the soft and hard diffractive processes can be obtained using combined measurements of TOTEM and CMS [20].

References

[1] D. M. Jansen, M. Albrow and R. Brugnera, hep-ph/9905537.

[2] R. Bonino et al., Phys. Lett. B 211 (1988) 239; A. Brandt et al., Nucl. Phys. B 514 (1998) 3.

[3] T. Ahmed et al., Phys. Lett. B 348 (1995) 681.

[4] M. Derrick et al., Z. Phys. C. 68 (1995) 569.

[5] C. Adloff et al., Z. Phys. C. 76 (1997) 613.

[6] L. Alvero et al., Phys. Rev. D 59 (1999) 074022.

[7] A. Hebecker and T. Teubner, hep-ph/0006234.

[8] G. Matthiae, talk given at the Workshop Diffraction 2000, Cetraro, Italy, 2-7 September 2000.

[9] S. M. Troshin and N. E. Tyurin, Phys. Part. Nucl. 30 (1999) 550.

[10] A. A. Logunov, V. I. Savrin, N. E. Tyurin and O. A. Khrustalev, Teor. Mat. Fiz. **6** (1971) 157;

[11] M. Baker and R. Blankenbecler, Phys. Rev. **128** (1962) 415.

[12] S. M. Troshin and N. E. Tyurin, Phys. Lett. **B 316** (1993) 175.

[13] P. M. Nadolsky, S. M. Troshin and N. E. Tyurin, Z. Phys. C **69** (1995) 131 .

[14] P. Desgrolard , L. Jenkovszky, B. Struminsky, Eur. Phys. J. C **11** (1999) 144.

[15] S.M. Troshin and N.E. Tyurin, Nuovo Cim. **106A** (1993) 327; Proc. of the Vth Blois Workshop on Elastic and Diffractive Scattering, Providence, Rhode Island, June 1993, p. 387; Phys. Rev. **D49** (1994) 4427; Z. Phys. C**64** (1994) 311.

[16] J. Velasco , J. Perez-Peraza, A. Gallegos-Cruz, M. Alvarez-Madrigal, A. Faus-Golfe, A. Sanchez-Hertz, hep-ph/9910484

[17] M. M. Block, F. Halzen and T. Stanev, hep-ph/9908222.

[18] C. Adloff et al., Eur. Phys. J. 1998 V. C10, 443 .

[19] S. M. Troshin and N. E. Tyurin, hep-ph/0008274.

[20] V. A. Petrov, talk given at the International Symposium " LHC Physics and Detectors", Dubna, 28-30 June 2000.